Polymer 49 (2008) 2866–2872

Contents lists available at ScienceDirect

Polymer

journal homepage: www.elsevier.com/locate/polymer

On the influence of the processing conditions on the performance of electrically conductive carbon nanotube/polymer nanocomposites

Nadia Grossiord [a,f], Patrick J.J. Kivit [a,f], Joachim Loos [b,c,f], Jan Meuldijk [d], Andriy V. Kyrylyuk [e,f], Paul van der Schoot [c,e,f], Cor E. Koning [a,f,*]

[a] Laboratory of Polymer Chemistry, Eindhoven University of Technology, Postbus 513, 5600 MB Eindhoven, The Netherlands
[b] Laboratory of Polymer Technology, Eindhoven University of Technology, Postbus 513, 5600 MB Eindhoven, The Netherlands
[c] Laboratory of Materials and Interface Chemistry, Eindhoven University of Technology, Postbus 513, 5600 MB Eindhoven, The Netherlands
[d] Process Development Group, Eindhoven University of Technology, Postbus 513, 5600 MB Eindhoven, The Netherlands
[e] Theoretical and Polymer Physics Group, Eindhoven University of Technology, Postbus 513, 5600 MB Eindhoven, The Netherlands
[f] Dutch Polymer Institute, P.O. Box 902, 5600 AX Eindhoven, The Netherlands

ARTICLE INFO

Article history:
Received 15 February 2008
Received in revised form 14 April 2008
Accepted 15 April 2008
Available online 24 April 2008

Keywords:
Nanocomposites
Conductivity
Processing conditions

ABSTRACT

We prepared multiwalled carbon nanotube/polystyrene (MWCNT/PS) nanocomposites using a latex-based process, the main step of which consists of directly mixing an aqueous suspension of exfoliated MWCNTs and a PS latex, both stabilized by an anionic surfactant. After freeze drying and compression molding homogeneous polymer films with well-dispersed carbon nanotubes were produced as evidenced by scanning electron microscopy. Conductivity measurements performed on our nanocomposite films show that they have a low percolation threshold and exhibit high levels of electrical conductivity above this threshold. We observe that both these properties are influenced by the applied processing conditions, i.e., temperature and time, and provide a plausible explanation based on the diffusive motion of the MWNTs in the polymer melt during the compression molding stage.

1. Introduction

Recently, much attention has been given to the use of carbon nanotubes (CNTs) as filler in conductive nanocomposites in order to harness their exceptional electrical properties [1,2]. CNTs are used as a dispersed conductive phase in an insulating polymer matrix. In the case of conductive nanocomposites, the target is to obtain a network of connected filler particles, which allow electrical current flow through the sample. In fact, the actual aim is to combine the "advantages" of both types of materials, i.e., the high conductivity of the CNTs with the good processability, low density, and so on, of polymeric materials. In the long term, these "conductive plastics" are expected to be able to replace metals or semiconductors for applications in which the latter are currently still preferred. Examples of such applications are electrostatic dissipation [3], electromagnetic interference shielding [4], multilayer printed circuits [5], and transparent conductive or antistatic coatings [6,7].

The electrical conductivity of composites consisting of a polymer matrix filled with conductive filler particles is usually discussed in terms of percolation theory [8–10]. The electrical conductivity of composites made of conductive filler particles dispersed in an insulating matrix strongly depends on the filler loading. At low filler concentrations the conductivity remains close to that of the electrically insulating matrix polymer because the filler particles are individually dispersed or grouped into small clusters. Above a critical filler volume fraction, the conductivity increases by many orders of magnitude over a small range in filler loading. This so-called percolation threshold coincides with the formation of a system spanning, conduction network of filler particles in the continuous polymer phase. Far above the percolation threshold, the conductivity of the nanocomposite levels off and does not increase significantly with the further addition of CNTs.

Interestingly, there is a considerable body of evidence for the presence of an insulating layer between the CNTs even above the percolation threshold, as in fact also seems to be the case for other types of conductive fillers including carbon black [11–19]. This then implies that the percolating filler particles are not in actual contact with each other, and that conductivity must occur via some tunneling or hopping process through the insulating layer that separates them. This can only happen if the shortest distance between two neighboring particles is below a certain value, estimated to be in the order of a couple of nanometers [20–22]. The type of electron transport involved should be strongly dependent on the CNT/polymer system in hand, and depends in particular on the statistics of inter-particle separations. It follows that the percolation

* Corresponding author. Laboratory of Polymer Chemistry, Eindhoven University of Technology, Postbus 513, 5600 MB Eindhoven, The Netherlands. Tel.: +31 40 247 2840; fax: +31 40 246 3966.
E-mail address: c.e.koning@tue.nl (C.E. Koning).

0032-3861/$ – see front matter © 2008 Elsevier Ltd. All rights reserved.
doi:10.1016/j.polymer.2008.04.033

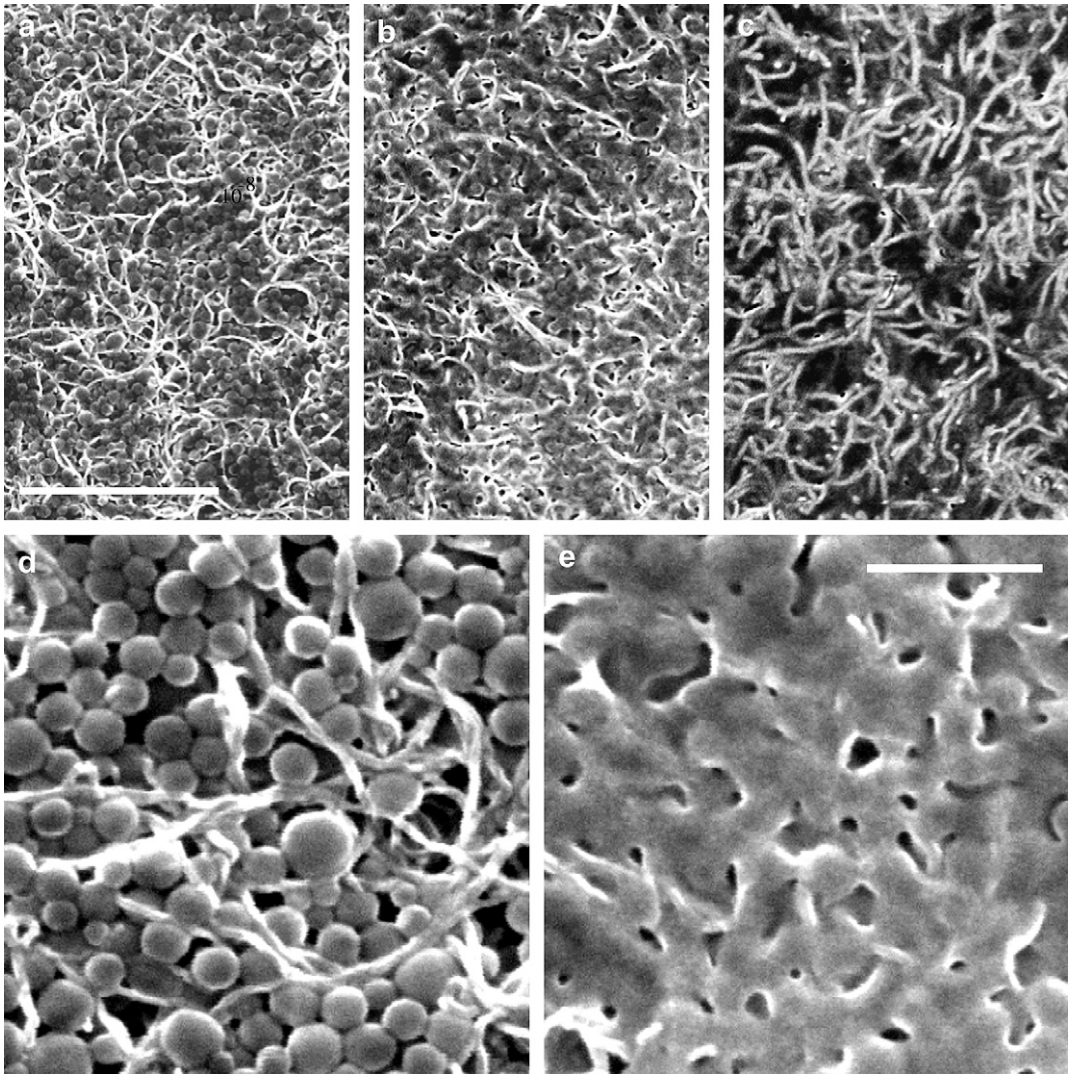

Fig. 1. SEM image of a freeze dried MWCNT/PS powder containing 7.8 wt% of MWCNTs (a) after heating at 60 °C, i.e., at a temperature at which no flow of the polymer takes place. The polymer particles are in a close-packed configuration and the CNTs are located in the interstitial space between them (b) after heating at 100 °C, the glass transition temperature of polystyrene. The polymer particles are deformed due to the polymer 'flow'; and (c) SEM surface image of the nanocomposite after processing at 180 °C, i.e., at a higher temperature than the flow temperature of the polymer. Scale bar for the three images (a–c) 1 μm; (d) detail of Fig. 1a. Scale bar: 200 nm; (e) detail of Fig. 1b. Scale bar for (d and e) 200 nm.

threshold is not only purely geometrically defined, as usually tacitly implied, but also physically defined, exactly because the particles need not quite touch for conduction to take place.

It is now clear that the percolation and conductivity of conductive nanocomposites are a sensitive function of the aspect ratio of the CNT filler particles [23,24], the degree of bundling and the polydispersity in size and shape [25–28], the interaction between the matrix and the filler and between the filler particles themselves [29], their average degree of orientation [30,31] and, interestingly, the conditions under which the composites are processed [32–34]. This last aspect is important because it means (i) that the measured percolation thresholds might not be the lowest possible for a given material system and (ii) that one should be weary comparing theoretical predictions that are often based on equilibrium percolation arguments [35,36]. The question of if and how equilibrium percolation is achieved in practice in nanocomposites seems to be a key one.

Here, we systematically address the problem of processing conditions on the percolation of electrically conductive CNT/polymer nanocomposites, produced by means of a latex-based technology [37,38]. The procedure that we follow comprises several steps. First, the CNTs are exfoliated or debundled in a surfactant solution by means of sonication [39,40]. The resulting aqueous surfactant–CNT dispersion is then mixed with an aqueous polymer latex. This is the key step of the process, because it determines how effective the incorporation of the CNTs into the polymer matrix is going to be. At this point, an equilibrium distribution is presumably regulated by the relative amounts of the rods and the latex particles and the way in which they interact. Then, the mixture of the two types of colloidal particles, i.e., the CNTs and latex particles, is freeze dried. In principle, the sublimation of the water induced by freeze drying is not expected to significantly modify the aggregated state of the CNTs nor the quality of mixing of the CNTs and the polymer latex particles. It seems that the CNT structure and quality are also not affected by this treatment [41]. Of course, freeze drying does induce a compaction of the CNT network that becomes denser because of the water removal.

After compaction of the powder consisting of submicron polymer particles and CNTs, the filler particles are forced into the interstitial space between the polymer latex particles [42,43]. The size distribution of the polymer particles governs the structure of the space where the fillers are confined, see Fig. 1a and d. Solvent removal and compaction do lead to an out-of-equilibrium

distribution of the CNTs because they cannot equilibrate. Provided the polymer particles are rigid and do not deform, the diameter of the polymer particles should strongly influence the way the CNTs permeate three-dimensional open space. If the powder obtained by freeze drying is compression molded at a temperature higher than the flow temperature of the polymer, the processing induces deformation and ultimately flow of the polymer (see Fig. 1a–e). The CNTs are then freed from the confinement in the interstitial space and in principle should be able to undergo diffusive motion in the polymer melt. This diffusive motion is driven by a thermodynamic driving force towards a new equilibrium state, which, if the polymer and CNTs mix well, should (in a way) be more random than the situation immediately after freeze drying. It is only after polymer melting that a new spatial distribution of CNTs can establish itself. Its structure is determined by the excluded volumes of the rods and by the effective CNT–CNT interaction caused by the coupling of the rods to the polymer melt. This coupling should in all likelihood introduce a weak attractive interaction between them, caused by the perturbation of the structure of the polymer melt.

It seems reasonable to assume that not only the size of the latex particles, which determines the initial structure of the composite, but also the viscosity of the polymer melt, which is a function of the molecular weight distribution, plays a role in the time it takes for the CNTs to attain their equilibrium structure in the melt. If the initial structure does not represent an electrically percolating network but the final equilibrium structure does, then the time allowed to the system to equilibrate should determine whether or not electrical percolation is actually achieved in the final product. This implies that the measured percolation threshold should be a function of the compression molding time and of the temperature at which the compression molding takes place, because the melt viscosity depends on the temperature. Finally, as already observed by Poetschke and her coworkers [34], the processing temperature should also has an impact on the final structure of the CNTs in any network, percolating or not, because the polymer-mediated effective interactions between the CNTs in the mixtures are plausibly temperature dependent. As it is now well established, the percolation threshold is a sensitive function of any interactions between the CNTs [25,43–45].

In this paper, we investigate the impact of the processing conditions on the percolation of the CNT network in the polymer matrix, and in particular the influence of the temperature and of the duration of compression molding step. Our study confirms the suggestion that diffusive processes are important and have to be considered when investigating percolation in nanocomposites involving polymeric materials. Our work also provides insight into the relevant structural reorganization time scales of CNTs in the polymer melt during compression molding after freeze drying.

2. Experimentals

2.1. Materials

Styrene (99%) and sodium carbonate (Na_2CO_3, 99%) were purchased from the Aldrich Chemical Co.; sodium dodecyl sulfate (SDS, 90%) and sodium persulfate (SPS) were provided by the Merck Chemical Co. MWCNTs were produced and kindly provided by Nanocyl Co (Belgium). They were made using a CVD-based process (thin MWCNTs Nanocyl-3100, batch 060213) and purified by the manufacturer by a mild non-oxidative acidic treatment. These CNTs were used as-received.

2.2. Instrumentation

All sonication processes were carried out with a horn sonicator of the type Sonic Vibracell VC750 with a cylindrical tip (10 mm end cap diameter). The frequency was fixed at (20 ± 0.2) kHz.

The molecular weight distribution of polystyrene (PS) studied was analyzed at 40 °C by Gel Permeation Chromatography (GPC) using a Waters Model 510 pump system with mixed packed columns preceded by a guard column PLgel mixC. Injections were done by a Waters Model WISP 712 auto/injector. Tetrahydrofuran (THF) was used as an eluent and the elution volumetric flow rate was maintained at 1.0 ml/min. The measurements were carried out with a refractive index detector, Waters Model 410, and a Model 486 UV detector operating at 254 nm. Data acquisition and processing were performed using Waters Millennium 32 (v3.2 or 4.0) software. Calibration was done using PS standards supplied by Polymer Laboratories, Inc. (USA).

Two-point and four-point conductivity measurements [46,47] were carried out with a Keithley 6512 Programmable Electrometer. Measurements were performed directly on the surface of the films. The contact between the sample and the measuring device was improved by the use of a colloidal graphite paste (Cat#12660) provided by Electron Microscopy Sciences (USA). Two- and four-point measurements should be equivalent to each other in the sense that they allow the determination of the resistivity (in Ω m, which is the inverse of the conductivity) of a given sample. Both types of measurements require the introduction of a test current into the specimen and the measurement of either a resistance or a resulting voltage. Four-point measurements are generally preferable over two-point measurements because the contact and spreading resistances introduced by the measuring are not taken into account in the specific contact resistance experimentally measured. However, since larger values of resistances are detectable with two-point measurements than with four-point measurements (see Ref. [47]), the formers allow a more precise characterization of the conductivity levels around the percolation threshold. That is why only the results obtained using the two-point measurements are explicitly shown in the present paper although both have been performed. The four-point measurements confirm our observations using the two-point measurements.

Morphological characterization of the as-prepared nanocomposites was performed using scanning electron microscopy [48]. The Scanning Electron Microscope (SEM, XL30 ESEM-FEG, Fei Co., The Netherlands) was equipped with a field-emission electron source. High vacuum conditions were applied and a secondary electron detector was used for image acquisition. The SEM was operated either in conventional high-voltage or low-voltage mode. No additional sample treatment such as surface etching or coating with a conductive layer was done. Standard acquisition conditions were as follows working distance of ~5 mm for low-voltage mode and ~10 mm for high-voltage charge contrast imaging, spot 3, slow-scan imaging with approximately 2 min/frame.

The low-shear viscosity of the polystyrene matrix materials was determined at 180 °C on a TA Instruments AR-G2 rheometer fitted with 25 mm stainless steel parallel plates.

2.3. Procedures

2.3.1. Exfoliation

MWCNTs (0.1 wt%) were mixed with 20 ml of an aqueous solution containing 0.2 wt% of SDS. The mixture was sonicated for 30 min at a power of 20 W with a horn sonicator, until maximum exfoliation was reached. The time of sonication and the CNT–surfactant mass ratio, necessary to achieve maximum exfoliation of the CNTs, were determined using a method based on UV–vis spectroscopy described elsewhere [39,49–51]. The aqueous dispersions were kept at a constant low temperature in an ice bath.

2.3.2. Emulsion polymerization

In order to synthesize the PS latex subsequently used to prepare the nanocomposites, a free radical emulsion polymerization was

carried out in an oxygen free atmosphere. Styrene (252 g) was mixed with 712 g of water in the presence of 26 g of sodium dodecyl sulfate (SDS) and 0.7 g of sodium carbonate (Na_2CO_3) buffer. The temperature of the mixture was brought to the reaction temperature, i.e., 70 °C. The polymerization was started by adding 0.7 g of sodium peroxide sulfate (SPS) dissolved in 5 g of demineralized water.

The polymer latex synthesized this way had a mean number average particle size of 85 nm as determined by Transmission Electron Microscopy (TEM). This polymer mainly contained high molar mass PS, i.e., above 10^6 g/mol. Its macroscopic viscosity was measured to be of the range of 10^6 Pa s at very low shear rates (lower than 1 s^{-1}).

2.3.3. Nanocomposites

The apparently stable surfactant–MWCNT dispersion obtained by sonication was first mixed with the PS latex. The whole mixture was then freeze dried (Chris Alpha 2–4). The resulting powder was transformed into films by compression molding (Collin Press 300G). The latter procedure consisted of a first short heating of the powder, without application of any pressure, in order to reach the desired working temperature. This heating was followed by a degassing step and two pressings at 40 bar for 20 s. The system was finally pressed at 100 bar at different temperatures, i.e., either 125 °C, 150 °C, or 180 °C, for various processing times, ranging from 2 min to 60 min.

3. Results and discussion

As one might infer from the introduction, one should strictly speaking distinguish between the actual percolation threshold and an apparent one, determined by the lowest CNT concentration needed for the nanocomposite to become conductive, regardless if the system has reached thermodynamic equilibrium or not. Formally, the actual percolation threshold is an intrinsic value of the percolating system considered, in our case CNTs dispersed in a PS matrix, because it is assumed to be in thermodynamic equilibrium when produced. In other words, the percolation threshold should not depend on the processing conditions [52]. As we shall see, the processing conditions can be chosen in such a way that the observed (or apparent) percolation threshold reaches a lower value, presumably equal to the intrinsic percolation threshold. For convenience, we will only use the term percolation threshold for both the intrinsic and the observed one. Note that this situation has to be contrasted to the percolation behavior of dispersed particles suddenly destabilized to such an extent that system spanning, kinetically arrested clusters form [53]. This is an interesting topic too but does not seem to apply to the type of system we are considering.

We pressed MWCNT/PS nanocomposites following the procedure described in the previous section at the three different temperatures 125 °C, 150 °C, and 180 °C. The last step of the compression molding lasted 2 min. The results of our conductivity measurements performed at the surface of these films are summarized in Fig. 2 and in Table 1 shown below. A visual determination of percolation thresholds from these curves lacks the desired accuracy. In order to determine the percolation thresholds as accurately as possible from the curves shown in Fig. 2 (and in Figs. 3 and 4), we took the midpoint between the last point giving the conductivity of the host polymer and the first point giving a significantly higher conductivity than the matrix due to percolation, namely the first point with a conductivity higher than 10^{-4} S/m. For this procedure, judging by the figures, we estimate an error of ca. ±10%. Although the number of points directly situated around the percolation threshold is limited, we also determined these thresholds by fitting the experimental data with the percolation theory. This approach yielded values which were, within

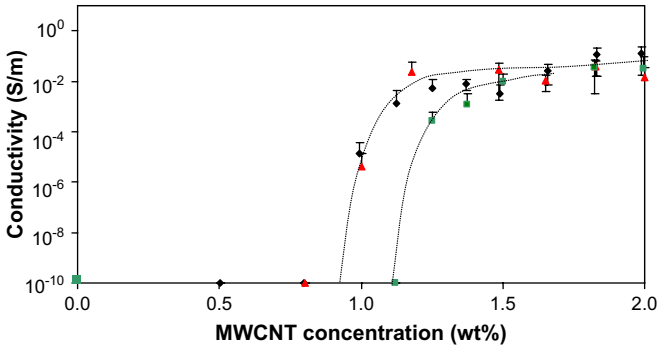

Fig. 2. Two-point conductivity measurements of MWCNTs/PS composites pressed for 2 min at 125 °C (■), 150 °C (▲) and 180 °C (◆). The dotted lines are guides for the eye and do not correspond to any theoretical fitting of the experimental data.

Table 1
Percolation threshold values (wt%) of the different series of nanocomposites with various processing times and temperatures. These values were obtained by taking the midpoint between the last point giving the conductivity of the host material and the first conductivity having a value above 10^{-4} S/m due to percolation

Processing conditions (t,T)	2 min	30 min	45 min	60 min
125 °C	1.25 ± 0.13	0.75 ± 0.08	0.81 ± 0.08	0.90 ± 0.09
150 °C	0.96 ± 0.10	0.75 ± 0.08		
180 °C	0.96 ± 0.10			

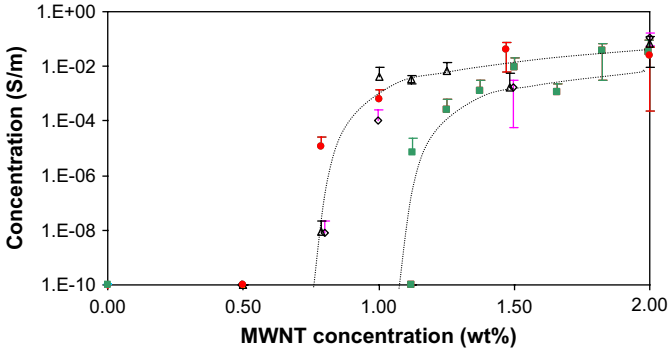

Fig. 3. Two-point conductivity measurements of MWCNT/PS composites pressed at 125 °C, for several processing times. The final pressing at 100 bar lasted: 2 min (■), 30 min (●), 45 min (△), and 60 min (◇). The dotted lines are guides for the eye and do not correspond to any theoretical fitting of the experimental data.

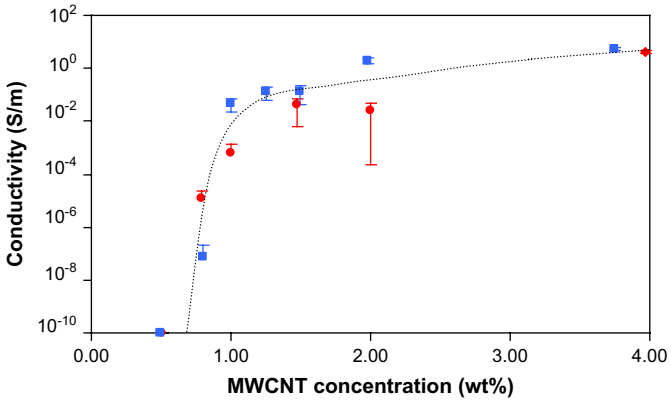

Fig. 4. Two-point conductivity measurements of MWCNT/PS composites processed for 30 min at 125 °C (●) and at 150 °C (■) in the final pressing step of 100 bar. The dotted line is a guide for the eye and does not correspond to any theoretical fitting of the experimental data.

experimental error, in excellent agreement with those obtained with the earlier mentioned 'midpoint' method. The values discussed here, and listed in Table 1, have been determined with the 'midpoint' method, and with respect to the aim of this paper seem to be accurate enough. We observe that the percolation threshold is strongly influenced by the processing temperature: after compression molding for 2 min at 125 °C the percolation threshold is around 1.2–1.3 wt% MWCNTs whilst at 150 °C and 180 °C the percolation thresholds are located between 0.9 wt% and 1.0 wt% MWCNTs (see Table 1). We find only minor differences in the conductivity levels between the different series at CNT loadings higher than 1.6 wt%. Near the percolation threshold, the composites pressed at 150 °C and 180 °C do display a significantly higher conductivity than those pressed at 125 °C. The conductivity of films containing 4 wt% of MWCNTs and processed at any of the three different temperatures was found to be about 15 S/m. So, at these high loadings, the molding temperature seems to be irrelevant.

If the equilibration time is an important factor determining the apparent percolation threshold, then increasing the processing temperature, given a constant processing time, or increasing the processing time at constant temperature should be equivalent. As already alluded to, increasing the temperature lowers the viscosity of the polymer matrix and through that the diffusivity of the CNTs. An increase of the diffusivity of the CNTs allows the system to evolve more quickly to its equilibrium state for a specific processing time. So, the higher the temperature is at which the nanocomposites are processed, the lower the percolation threshold is, albeit that there is a lower bound, being the actual (equilibrium) percolation threshold. The results of Fig. 2 are in accord with this expectation.

If, on the other hand, the processing time is varied at constant temperature and the system needs a minimum amount of time to equilibrate by diffusion of the CNTs, then below a certain processing time it cannot reach the actual percolation threshold. It is important to realize that the time required to reach equilibrium is not an invariant of the loading of the CNTs, firstly because it depends on the strength of the thermodynamic driving force, i.e., how far the system is removed from equilibrium at time zero, and secondly because the diffusivity of the CNTs could depend on the concentration. The reason is that the CNTs should be strongly entangled under conditions where percolation takes place [54]. See, however, below.

The equivalence of the impact of processing temperature and time was verified experimentally by conductivity measurements performed on a series of composites pressed at 125 °C for a range of processing times. The results for processing times of 2 min, 30 min, 45 min and 60 min are shown in Fig. 3 (See also Table 1). When the nanocomposites were processed for a short period of time, say, 2 min, then the observed percolation threshold is around 1.2 wt% MWCNTs. It shifts to lower values if the processing time is increased, and reaches a minimum value of about 0.75–0.90 wt% MWCNTs if processed for 30 min or longer. This minimum value must represent the equilibrium percolation threshold and is (given the estimated error of ca. ±0.1 wt%) quite close to the corresponding threshold that was found by varying the processing temperature (shown in Fig. 2), as it should.

Fig. 4 shows our conductivity curves obtained for the series of composites pressed at the two temperatures of 125 °C or 150 °C for 30 min, and they turn out to be not significantly different from each other. They also agree well with the results shown in Fig. 2. The percolation threshold derived from Fig. 4, using the earlier mentioned 'midpoint method', is also around 0.8–0.9 wt%. This confirms that the system has certainly reached its equilibrium state under these processing conditions.

An important observation is that the conductivity of nanocomposites at higher MWCNT loadings of, say, 4 wt%, turns out to be similar for all the nanocomposites prepared, regardless of the conditions at which they were processed. This confirms our suggestion that the equilibration time is not an invariant of the particle loading. In fact, the higher the concentration the stronger the thermodynamic driving force, the shorter the equilibration time should be. On the other hand, for higher CNT concentrations this effect might be hindered by a congestion-induced reduction of the self-diffusivity of the CNTs [54].

In order to facilitate the comparison between the different sets of experiments and to provide the reader an overview of our results, the observed percolation thresholds for the different series of nanocomposites prepared are collected in Table 1. As mentioned earlier, these values were obtained by taking the midpoint between the last point giving the conductivity of the host material and the first conductivity having a value above 10^{-4} S/m due to percolation.

Although we have not investigated the impact of the processing conditions on single-walled carbon nanotubes dispersed in a polymer matrix, it is tempting to speculate on how the CNT diameter impacts on the percolation threshold. Let us in a 'theoretical experiment' consider two series of nanocomposites prepared either with SWCNTs or with MWCNTs of identical length distribution. SWCNT diameters are typically slightly below 1 nm, whereas the diameters of MWCNTs are quite a bit larger and 20 nm on average for the MWNTs used in our study. As mentioned earlier, the percolation threshold is inversely proportional to the aspect ratio of the CNTs. As a result, in the simplified case in which CNTs would behave like non-interacting rigid rods, it follows that the percolation threshold of the SWCNT-based nanocomposites should be at least 10× smaller than the one of the MWNT-based nanocomposites. Here, we account for the fact that the densities of SWNTs and MWNTs are typically 1500 kg/m^3 and 1800–2100 kg/m^3 depending on the characteristics of the MWCNTs.

To the best of our knowledge, there is no kinetic version of the connectedness percolation theory. However, there is a formal correspondence between the statistical theory of the equilibrium structure of fluid dispersions and the static connectedness percolation theory of dispersed particles [25,55]. Presuming that the same correspondence also holds out of equilibrium, we might get in this way an estimate for the time that it takes for the network to restructure during the processing.

In the static case, this correspondence amounts to equating the static structure factor of the particles in the limit of vanishing wave vector to the mean cluster size S, and replacing the so-called direct correlation function by its connectedness counterpart. For rods, the static structure factor can be calculated quantitatively for large aspect ratios because the second virial approximation then holds [54,56]. This gives a mean cluster size $S = (1 - \phi/\phi_p)^{-1}$ that diverges when the loading fraction ϕ equals the percolation threshold ϕ_p, which is inversely proportional to the aspect ratio of the rods. For $\phi > \phi_p$ this expression no longer holds, as S is infinite in that case.

To get the kinetic equivalent, we equate the dynamical structure factor in the limit of vanishing wave vector to the dynamical equivalent of the cluster size $S(t)$ at time t, and again apply the second virial theory [56].

$$S(t) = S(0)\exp\left[-Dq_{\min}^2\left(1-\frac{\phi}{\phi_p}\right)t\right] \quad (1)$$

where D is the mean of the parallel and perpendicular translational self-diffusion constants of the rods and $S(0) = S$ the equilibrium value of the cluster size at time $t = 0$, presumed to be finite. We have retained in Eq. (1) the lowest order term in powers of the smallest wave vector $q_{\min} \approx 2\pi/l$ allowed by the system size l. (The system size should be of the order of the distance between the electrodes.) Eq. (1) is strictly speaking valid for short times only, but this will do for our purpose.

For $\phi < \phi_p$ the quantity $S(t)$ relaxes to zero because rods detach and attach so that after some time set by Eq. (1) it has renewed itself completely. For $\phi > \phi_p$, $S(t)$ increases with time, a result of the cluster growth. The amount of time τ it takes to span the system depends on the system size l, the initial size S, the diffusivity D and how deeply we have quenched the system beyond the percolation threshold. From Eq. (1) we deduce that a crude estimate for this time would obey:

$$\tau^{-1} \approx Dq_{\min}^2 \left| 1 - \left(\frac{\phi}{\phi_p} \right) \right| \quad (2)$$

Eq. (2) tells us that the equilibration time should decrease with increasing particle loading, at least if D is only weakly concentration dependent. This is the result of a thermodynamic driving force for network re-structuring that increases with loading. It has the same origin as the increased driving force for the equilibration of spontaneous density variations at higher densities of particles [54].

Note that, according to Eq. (2), exactly at the percolation threshold, where $\phi = \phi_p$, it takes an infinite amount of time to establish the percolating network, a phenomenon equivalent to the critical slowing down near the spinodal of phase separating systems [54]. For $\phi > \phi_p$ this amount of time remains finite but should still be very large, unless the cluster size at time zero is close to the system spanning. Unfortunately, because there is no reliable theory allowing us to calculate the diffusivity D for entangled rods in a polymeric fluid, there is little hope at this point of getting a reasonable estimate for the relaxation time. As we already indicated, D could be a function of the loading ϕ but it may also well be that the entanglement of the CNTs by the polymer molecules in the matrix predominates.

Indeed, in our case the rods are highly entangled by the PS matrix of high molecular weight polymer, in fact much higher than the critical entanglement molar weight of 35,000–38,000 g/mol [57,58]. Hence, the motion perpendicular to the CNT axis should almost completely be suppressed whilst the motion parallel to it could well be largely unhindered by the effects of entanglement [58]. If that is the case, we surmise that D must inversely proportional to the local viscosity of the matrix, i.e., the viscosity experienced by the nanotubes [54]. This viscosity should be much lower than the macroscopic viscosity, which we established to be about 3.3×10^4 Pa s, because the latter is dominated by the effects of entanglement.

Although we cannot directly verify Eq. (2) against the experiments, a few important conclusions can nevertheless be drawn from it. Eq. (2) tells us that the equilibration time is a function of the loading, of the viscosity and, hence, of the temperature. This seems to be in agreement with the measurements, as already discussed. If the equilibration time is fixed and the loading increased, there is a minimal loading where equilibrium can be reached within the allowed processing time. This critical loading must, according to Eq. (2), be larger than the actual percolation threshold. Beyond the critical loading the conductivity should become an invariant of preparation conditions. The results of Fig. 3 bear this out.

At constant processing time but at increasing temperature the equilibration time decreases until at some point the latter drops below the processing time, and equilibration can take place. So, above a critical temperature the conductivity should become an invariant of the temperature. This is not quite true of course, because the temperature affects the percolation threshold too, as it does the conductivity itself. The results of Fig. 2 agree qualitatively with this conclusion.

In conclusion, our experiments strongly support the idea that the compression molding step allows for the diffusive reorganization of the CNTs in the polymer matrix. It allows the in a way "frustrated" organization of the CNTs in the interstitial space between the intact PS latex particles, obtained after freeze drying, to relax. For comparable CNT/latex systems for which no polymer flow occurs during the film formation, such as described by Grunlan and his coworkers [42], the CNTs stay confined in the interstitial volume between the polymer particles. In that case, the percolation behavior of the CNTs is strongly affected by the particle size of the polymer matrix and the CNT network obtained after water evaporation will be similar to the one of the final film. As shown here, provided sufficiently high temperatures are used and a sufficient amount of time is given to the CNTs to reorganize and to reach the equilibrium state in the final compression molding step, the particle size of the polymer latex used should have a very limited impact on the electrical conductivity of the nanocomposite.

4. Summary and conclusions

We have shown that it is possible to efficiently and homogeneously disperse CNTs into a polymer matrix by means of a latex-based preparation procedure. CNT/PS nanocomposites prepared by this versatile and environmentally friendly method display remarkable electrical properties, that is, a very low percolation threshold and a high level of conductivity above that.

Before the melt processing step of the procedure, the system consists of a powder of closely-packed vitrified latex particles mixed with CNTs. The latter are confined in the interstitial spaces between the polymer particles. In the final compression molding step the polymer melts, allowing the CNTs to in principle reorganize by diffusion in the polymer melt.

The viscosity of the polymer matrix determines to what extent the CNTs can reorganize within a given amount of time, because it determines the diffusivity of the CNTs in it. It is, up to a point, a controllable parameter, as it depends on the kind of polymer used, its molar mass distribution and on the processing temperature.

Notably, changing the processing conditions, such as enhancing the temperature and the time of compression, lowers the percolation threshold and raises the conductivity of the nanocomposite by pushing the system towards its equilibrium state. So, as long as sufficiently high temperatures are used and enough time is given to the system to reach its equilibrium, the particle size of the polymer latex is expected to have a limited impact on the electrical conductivity of the nanocomposite.

Acknowledgements

The research described in this article is part of the research programme of the Dutch Polymer Institute, DPI project #416. The authors would like to thank Hans Miltner (Free University of Brussels) for performing the viscosity measurements, as well as Nanocyl for supplying the carbon nanotubes used in the present study.

References

[1] Wildoer JWG, Venema LC, Rinzler AG, Smalley RE, Dekker C. Nature 1998;391:59–61.
[2] Odom TW, Huang J, Kim P, Lieber CM. Nature 1998;391:62–4.
[3] Hyperion Catalysis International. Plast Add Comp September 2001;3:20–2.
[4] Kim W-S, Song HS, Lee BO, Kwon K-H, Lim Y-S, Kim M-S. Macromol Res 2002;10:253–8.
[5] Shibayama K, Nakasuga A. Japan, Patent number JP 2004075706; 2004.
[6] Wu Z, Chen Z, Du X, Logan JM, Sippel J, Nikolou M, et al. Science 2004;305:1273–6.
[7] Kong B-S, Jung D-H, Oh S-K, Han C-S, Jung H-T. J Phys Chem C 2007;111:8377–82.
[8] Kirkpatrick S. Rev Mod Phys 1973;45(4):574–88.
[9] Dufresne A, Paillet M, Putaux JL, Canet R, Carmona F, Delhaes P, et al. J Mater Sci 2002;37:3915–23.
[10] Balberg I, Azulay D, Toker D, Millo O. Int J Mod Phys B 2004;18:2091.
[11] Kilbride BE, Coleman JN, Fraysse J, Fournet P, Cadek M, Drury A, et al. J Appl Phys 2002;92(7):4024–30.

[12] Kymakis E, Amaratunga GAJ. J Appl Phys 2006;99:084302.
[13] Kim HM, Choi M-S, Joo J. Phys Rev B 2006;74:054202.
[14] Kim YJ, Shin TS, Choi HD, Kwon JH, Chung Y-C, Yon HG. Carbon 2005;43:23–30.
[15] Sandler JKW, Kirk JE, Shaffer MSP, Windle AH. Polymer 2003;44:5893–9.
[16] Barrau S, Demont A, Laurent C, Lacabanne C. Macromolecules 2003;36:5187–94.
[17] Connor MT, Roy S, Ezquerra TA, Baltá Calleja FJ. Phys Rev B 1998;57(4):2286–94.
[18] Alexander MG. Mater Res Bull 1999;34(4):603–11.
[19] Sichel EK, Gittleman JI, Sheng P. Phys Rev B 1978;18(10):5712–6.
[20] Strümpler R, Glatz-Reichenbach J. J Electroceram 1999;3(4):329–46.
[21] Rubin Z, Sunshine A, Heaney MB, Bloom I, Balberg I. Phys Rev B 1999;59(19):12196–9.
[22] Sichel EK, Gittleman JI, Sheng P. J Electron Mater 1982;11(4):699–747.
[23] Yi JY, Choi GM. J Electroceram 1999;3:361–9.
[24] Hecht D, Hu L, Grüner G. Appl Phys Lett 2006;89:133112.
[25] Kyrylyuk AV, Van der Schoot P. Proc Natl Acad Sci, in press.
[26] Bryning MB, Islam MF, Kikkawa JM, Yodth AC. Adv Mater 2005;17:1186–91.
[27] Baughman RH, Zakhidov AA, de Heer WA. Science 2002;297:787.
[28] Schmidt RH, Kinloch IA, Burgess AN, Windle AH. Langmuir 2007;23:5707–12.
[29] Miyasaka K, Watanabe K, Jojima E, Aida H, Sumita M, Ishikawa K. J Mater Sci 1982;17:1610–6.
[30] Munson-McGee SH. Phys Rev B 1991;43:3331–6.
[31] Du F, Fischer JE, Winey KI. Phys Rev B 2005;72:121404(R).
[32] Dalmas F, Cavaille J-Y, Gauthier C, Chazeau L, Dendievel R. Compos Sci Technol 2007;67:829–39.
[33] Kim YS, Wright JB, Grunlan JC. Polymer 2008;49:570–8.
[34] Villmow T, Pegel S, Poetschke P, Wagenknecht U. Compos Sci Technol 2008;68:777–89;
Pegel S, Poetschke P, Petzold G, Alig I, Dudkin SM, Lellinger D. Polymer 2008;49:974–84.
[35] Lux F. J Mater Sci 1993;28:285–301.
[36] Zakri C, Poulin P. J Mater Chem 2006;16:4095–8.
[37] Grossiord N, Loos J, Koning CE. J Mater Chem 2005;15:2349–52.
[38] Regev O, ElKati PNB, Loos J, Koning CE. Adv Mater 2004;16:248–51.
[39] Grossiord N, Regev O, Loos J, Meuldijk J, Koning CE. Anal Chem 2005;77:5135–9.
[40] Vigolo B, Penicaud A, Coulon C, Sauder C, Pailler R, Journet C, et al. Science 2000;290(5495):1331–4.
[41] Maugey M, Neri W, Zakri C, Derre A, Penicaud A, Noe L, et al. J Nanosci Nanotechol 2007;7(8):2633–9.
[42] Grunlan JC, Mehrabi AR, Bannon MV, Bahr JL. Adv Mater 2004;16:150–3.
[43] Malliaris A, Turner DT. J Appl Phys 1971;42(2):614–8.
[44] Vigolo B, Coulon C, Maugey M, Zakri C, Poulin P. Science 2005;309:920–3.
[45] Bug ALR, Safran SA, Grest GS, Webman I. Phys Rev Lett 1985;55(18):1896–9.
[46] Posthumus W. UV-curable acrylate metal oxide nanocomposite coatings. Ph.D. thesis. Eindhoven: Eindhoven University of Technology; 2004.
[47] Wentworth SM. Charact Mater 2003;1:401–11.
[48] Loos J, Alexeev A, Grossiord N, Koning CE, Regev O. Ultramicroscopy 2005;104:160–7.
[49] Yu J, Grossiord N, Koning CE, Loos J. Carbon 2007;45:618–23.
[50] Grossiord N, Miltner HE, Loos J, Meuldijk J, van Mele B, Koning CE. Chem Mater 2007;19:3787–92.
[51] Grossiord N, van der Schoot P, Meuldijk J, Koning CE. Langmuir 2007;23(7):3646–53.
[52] Kovacs JZ, Velagala BS, Schulte K, Bauhofer W. Compos Sci Technol 2007;67:922–8.
[53] Michels MAJ, Brokken-Zijp JCM, Groenewoud WM, Knoester A. Physica A 1989;157:529–34.
[54] Doi M, Edwards SF. The theory of polymer dynamics. Oxford Science Publications; 1986.
[55] Coniglio A, De Angelis V, Forlani A. J Phys A Math Gen 1977;10:1123–39.
[56] Doi M, Shimada T, Okano KJ. Chem Phys 1988;88:4070–5.
[57] Sperling LH. Introduction to physical polymer science. Chichester: Wiley-Interscience; 2001.
[58] Majeste JC, Montfort JP, Allal A, Marin G. Rheol Acta 1998;37:486–99.